

Porous polymeric ligand promoted copper-catalyzed C-N coupling of (hetero)aryl chlorides under visible-light irradiation

Erfei Wang¹, Kaixuan Chen¹, Yinan Chen¹, Jiawei Zhang², Xinrong Lin^{2*} & Mao Chen^{1*}

¹State Key Laboratory of Molecular Engineering of Polymers, Department of Macromolecular Science, Fudan University, Shanghai 200438, China;

²Key Laboratory of Medicinal Chemistry for Natural Resource, Ministry of Education and Yunnan Province, School of Chemical Science and Technology, Yunnan University, Kunming 650091, China

Received July 13, 2020; accepted August 25, 2020; published online October 29, 2020

A porous polymeric ligand (PPL) has been synthesized and complexed with copper to generate a heterogeneous catalyst (Cu@PPL) that has facilitated the efficient C-N coupling with various (hetero)aryl chlorides under mild conditions of visible-light irradiation at 80 °C (58 examples, up to 99% yields). This method could be applied to both aqueous ammonia and substituted amines, and is compatible to a variety of functional groups and heterocycles, as well as allows tandem C-N couplings with conjunctive dihalides. Furthermore, the heterogeneous characteristic of Cu@PPL has enabled a straightforward catalyst separation in multiple times of recycling with negligible catalytic efficiency loss by simple filtration, affording reaction mixtures containing less than 1 ppm of Cu residue.

polymeric catalyst, heterogeneous catalysis, photocatalysis, C-N coupling

Citation: Wang E, Chen K, Chen Y, Zhang J, Lin X, Chen M. Porous polymeric ligand promoted copper-catalyzed C-N coupling of (hetero)aryl chlorides under visible-light irradiation. *Sci China Chem*, 2020, 63, <https://doi.org/10.1007/s11426-020-9859-9>

The development of versatile synthetic methods for the formation of carbon-nitrogen (C–N) bonds can impact the fields of pharmaceutical [1,2], agrochemical [3,4] and natural-product synthesis [5,6], as well as material science [7,8]. Consequently, a variety of synthetic strategies promoted by transition-metal catalysis including Buchwald-Hartwig [9,10] and Ullmann [11,12] coupling reactions, have been developed. Despite the extraordinary advances accomplished with these diverse and robust reaction systems, attaining desirable reaction characteristics such as mild conditions (*i.e.*, Ullmann coupling requires temperature above 180 °C), straightforward catalyst separation, as well as bond activation upon more economically competitive substrates, remains challenges confronting researchers in pursuit of enhanced sustainability and operational utility of the

chemistry [13,14].

Heterogeneous catalysts have received increasing attention owing to their unique attribute of being recycled at ease [15–17], which may carry important cost implications in industrial chemical manufacturing, and have promoted synthetic transformations ranging from hydrogenation [18], enyne cyclization [19] to Suzuki-Miyaura coupling [20]. While heterogeneous catalysis could provide an attractive and convergent approach to form C–N bond between nitrogen nucleophiles and (hetero)aryl halides and access a broad scope of N-containing molecules, such transformation processes generally suffer from (1) decreased reactivity with non-noble copper catalysts and aryl chlorides; (2) limited tolerance to functional groups and heterocycles [21,22]. Furthermore, as equally challenging in homogeneous catalysis, the direct amination with (hetero)aryl chlorides and ammonia/amines has been rarely possible with hetero-

*Corresponding authors (email: xrlin@ynu.edu.cn; chenmao@fudan.edu.cn)

geneous catalysts arising from the insufficient reactivity of (hetero)aryl chlorides.

Beyond heterogeneous catalysts, Fu and co-workers [23,24] have developed the photoinduced Ullmann C–N coupling under mild conditions, which allowed the transformation of electrophiles including aryl bromides/iodides. Visible-light has also promoted other bond formations [25–28]. Nevertheless, the utilization of aryl chlorides is still difficult [29]. Ma and co-workers [30–32] have recently made new breakthroughs in the Cu-catalyzed Ullmann-type reaction of aryl chlorides. Upon applying elevated reaction temperatures (110–130 °C) and making structural modifications based on the oxalamide ligand backbones, good catalytic activities were achieved for the coupling reactions between different types of nitrogen nucleophiles (*i.e.*, ammonia and alkyl amine) and aryl chlorides.

We hypothesize that a heterogeneous system based on a versatile and light-absorbing polymeric Cu-complex might facilitate the C_{aryl}–Cl bond cleavage *via* a photoinduced process [23], thereby broadening the applicable scope of Cu-catalyzed Ullman reaction at lower reaction temperatures and simultaneously facilitating straightforward catalyst separation/recycling. Meanwhile, the highly porous morphology of the polymeric catalyst could effectively increase the accessible surface area and suppress the catalytic efficiency decay. Herein, we report that a novel porous polymeric ligand (PPL) was synthesized and coordinated with copper to generate a heterogeneous catalyst (Cu@PPL), promoting a general and efficient C–N bond formation between a broad scope of (hetero)aryl chlorides and ammonia/alkyl amines with good to excellent yields (58 examples, up to 99% yields). This catalyst enabled a decrease in required reaction temperature for as high as 40 °C when exposing to visible-light irradiation (Figure 1). Furthermore, the heterogeneous catalyst exhibited facile recyclability and excellent stability, which results in repeated use in the reactions without diminishing its catalytic efficiency.

At the beginning of the investigation, polymeric ligands **L1**–**L6** were synthesized *via* condensation polymerization of oxalyl chloride and diamine compounds, and complexed with CuI to generate heterogeneous catalysts of Cu@Ligand. The Cu-catalyzed C–N bond formation between 4-*n*-butylchlorobenzene and aqueous ammonia was employed as a model reaction using K₃PO₄ as a base in dimethyl sulfoxide (DMSO). As shown in Table 1, when complexes made of polymeric ligands **L1**–**L6** were employed, the reactions generated 4-*n*-butylaniline **1** at 12%–36% yields at 120 °C in 24 h as determined by gas chromatography (GC) analysis (entries 1–6).

When the reactions between 4-*n*-butylchlorobenzene and ammonia were exposed to visible-light irradiation with white light-emitting diode (LED) light (10 W), clearly improved yields of 4-*n*-butylaniline were obtained at decreased reac-

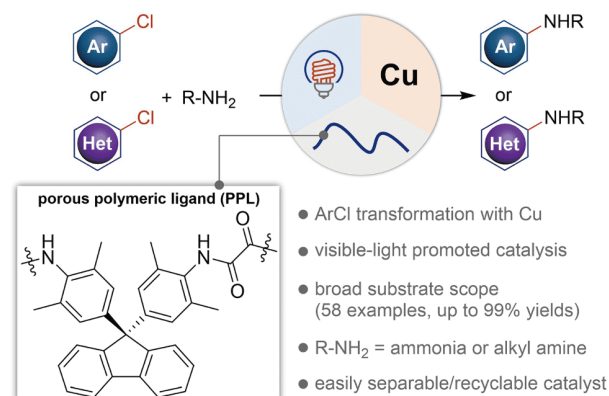


Figure 1 Cu-catalyzed C–N bond formation under visible-light irradiation with oxalamide-linked porous polymeric ligand (PPL) (color online).

Table 1 C–N bond formation between 4-*n*-butylchlorobenzene and aqueous ammonia^{a)}

Entry	Ligand	Light irradiation	Temperature (°C)	Time (h)	Yield ^{b)}
1	L1	No light	120	24	15
2	L2	No light	120	24	32
3	L3	No light	120	24	12
4	L4	No light	120	24	29
5	L5	No light	120	24	18
6	L6	No light	120	24	36
7	L6	White light	100	24	76
8	L6	405 nm	100	24	92
9	L6	405 nm	80	48	>99 (99) ^{c)} , 82 ^{d)}
10	L6	405 nm	60	48	56
11	L6	405 nm	80	48	27–85 ^{e)}
12	L6	405 nm	80	48	88 ^{f)}

a) Conditions: 4-*n*Bu–Ph–Cl (0.5 mmol), aqueous ammonia (1 mmol), Cu@Ligand (0.05 mmol), K₃PO₄ (0.6 mmol), DMSO (0.5 mL). b) GC yield. c) Isolated yield in parentheses. d) 24 h. e) When DMF, DMAc or *t*BuOH was used instead of DMSO, yield was 82%, 75% and 27%, respectively; when Cs₂CO₃, K₂CO₃ or Na₂CO₃ was used instead of K₃PO₄, yield was 85%, 54% and 36%, respectively. f) 5 mol% Cu@**L6**.

tion temperature (100 °C). Among polymeric ligands of **L1** to **L6**, the employment of **L6** (PPL) afforded the highest GC

yield (76%, entry 7, Table S1, [Supporting Information online](#)), which was further improved to >99% at even lower temperature (80 °C) by using a purple LED light (emission at 405 nm, 10 W, entry 9). Subsequently, lower reaction temperatures (*i.e.*, 60 °C), other solvents (*i.e.*, *N,N*-dimethylformamide (DMF), DMAc and *n*BuOH) and bases (*i.e.*, Cs₂CO₃, K₂CO₃, Na₂CO₃) were investigated with Cu@L6, providing 27%–85% yields of 4-*n*-butylaniline (entries 10–11) in 48 h irradiation time. When 5 mol% catalyst was used, 88% yield was obtained (entry 12).

Subsequently, L6 and Cu@L6 were characterized by a variety of measurements. In the Fourier transform infrared (FT-IR) spectra ([Figure 2\(a\)](#)), the signals in the range from 1,750–1,650 and 3,450–3,250 cm⁻¹ were attributed to the vibration of the C=O and N–H bonds, respectively, indicating the formation of amide during the condensation polymerization, and suggesting that the polymer's backbone was retained during the coordination with copper. When analyzed by ultraviolet-visible (UV-Vis) spectroscopy ([Figure 2\(b\)](#)), the copper complex gave the strongest adsorption at 410 nm in the visible-light range, which was consistent with the emission wavelength of LED employed in the coupling reaction. As shown in [Figures 2\(c1, c2\)](#), the formation of copper complex also caused a color change from light purple to brown. The high thermal stability of L6 and Cu@L6 were confirmed by thermo-gravimetric analysis (TGA), affording 5% mass loss at 372 and 395 °C, respectively ([Figure S3, Supporting Information online](#)). Brunauer-Emmett-Teller (BET) measurement was used to study the porosity of L6 and Cu@L6 by analyzing the N₂ adsorption and desorption isotherms ([Figure 2\(d\)](#)). In comparison to L6, a smaller surface area of Cu@L6 was detected (396 *vs.* 237 m²/g), resulted from partial occupation of the porous structure by the introduced Cu. The hierarchically porous property was also proven by the pore size distribution according to the nonlocal density functional theory (NLDFT) [33]. The results shown in [Figure 2\(e\)](#) demonstrated the presence of narrowly distributed pore sizes of about 2 and 5 nm, representing mixed micropores and mesopores of Cu@L6, which is advantageous for heterogeneous catalysis owing to the excellent adsorption of substrates and efficient mass transport of products that could be provided by porous carriers. When analyzed by scanning electron microscopy (SEM), corresponding images ([Figure 2\(f, g\)](#)) displayed distinctive morphologies of porosity for L6 and Cu@L6. The high-resolution transmission electron microscopy (HR-TEM) images of L6 and Cu@L6 ([Figure 2\(h, i\)](#)) showed their amorphous structures and the well dispersity of Cu in the matrix. Otherwise, when L6 and Cu were mixed at their solid states, Cu nanoparticles are clearly observed by HR-TEM as confirmed by the lattice fringes with a spacing distance of 0.21 nm ([Figure S3](#)) [34]. Additionally, scanning transmission electron microscopy (STEM) and element mapping

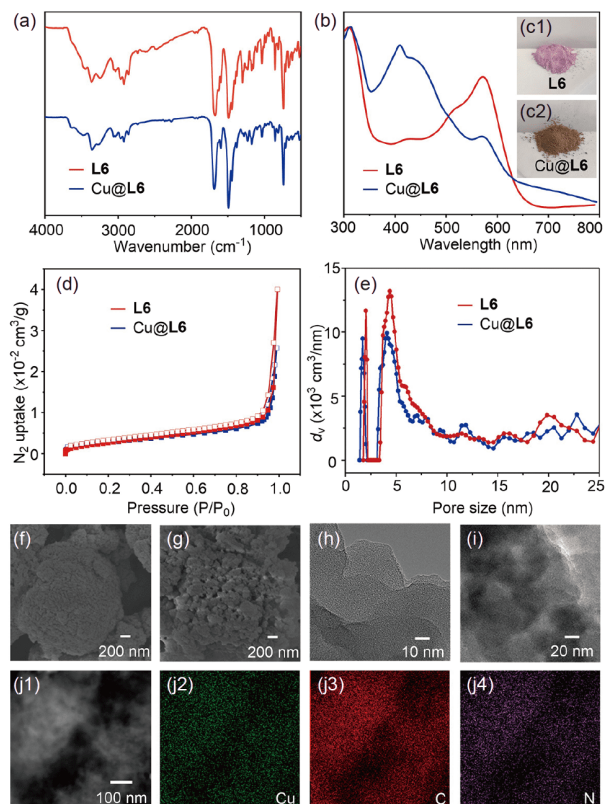
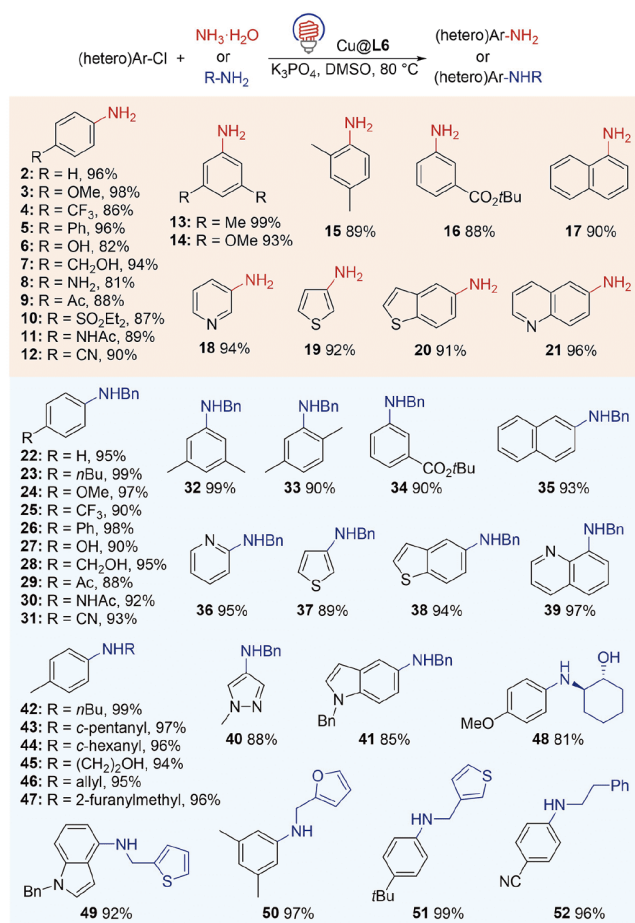


Figure 2 Characterization of L6 and Cu@L6. (a, b) FT-IR and UV-Vis spectra; (c) optical images; (d) adsorption (filled symbols) and desorption (empty symbols) isotherms recorded under N₂ atmosphere; (e) pore size distribution obtained by NLDFT; (f, g) SEM images of L6 and Cu@L6, respectively; (h, i) HR-TEM images of L6 and Cu@L6, respectively; (j1) STEM image of Cu@L6; (j2–j4) element mapping images of Cu@L6 based on (j1) (color online).

images of Cu@L6 ([Figure 2\(j1–j4\)](#)) further confirm that the Cu, C and N elements were evenly dispersed on the polymeric support, which prompts efficient catalytic process.

With the optimized conditions, we investigated the substrate scope of the photo-promoted Cu-catalyzed C–N coupling between (hetero)aryl chlorides and nitrogen nucleophiles. As shown in [Scheme 1](#), for nucleophiles of both aqueous ammonia and substituted amines, the coupling could be successfully carried out with *para*-, *meta*-, and *ortho*-substituted aryl compounds and fused aryl substrates at 80 °C; electron-rich, electron-neutral, and electron-deficient aryl chlorides all represented excellent substrates. Moreover, the reaction condition tolerated a variety of functional groups including unprotected hydroxyl (**6**, **7**, **27**, **28**), amine (**8**), acetyl (**9**, **29**), sulfamide (**10**), amide (**11**, **30**), nitrile (**12**, **31**) and ester (**16**, **34**).

While heteroaryl amines have shown profound research value for their biological activity [35,36], the copper-catalyzed reactions for this class of substrates remain challenging due to the proneness of heterocycles to coordinate to copper species [37,38]. With this method, a variety of heterocyclic compounds including pyridine (**18**, **36**), thiophene (**19**, **37**),



Scheme 1 Cu@L6 Catalyzed C-N Coupling between (Hetero)aryl chlorides and ammonia/amines. Conditions: (hetero)aryl chloride (0.5 mmol), aqueous ammonia (1 mmol) or R-NH₂ (0.6 mmol), Cu@L6 (0.05 mmol), K₃PO₄ (0.6 mmol), DMSO (0.5 mL), 80 °C, visible light at 405 nm, 48 h. Isolated yields are based on electrophiles (color online).

thionaphthen (**20**, **38**), quinoline (**21**, **39**), pyrazole (**40**) and indole (**41**) could be efficiently coupled with ammonia or amines under light-irradiated heterogeneous conditions.

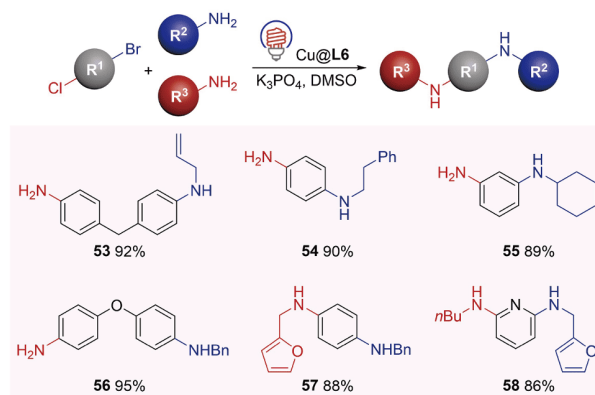
In terms of amines, the tolerated substituent groups could not only include benzyl (**22–41**), a protecting group usually employed in organic synthesis, but also comprise *n*-alkyl (**42**), cyclic alkyl (**43**, **44**), hydroxyl substituted alkyl (**45**, **48**), allyl (**46**), 2-furanylmethyl (**47**, **50**), 2-thienylmethyl (**49–51**) and phenethyl (**52**) groups. Taken together, this method exhibited a good substrate scope for both (hetero)aryl chlorides and nitrogen nucleophiles, enabling the generation of target products in good to excellent yields (81%–99%) under mild conditions.

Tandem reactions from conjunctive dihalide electrophiles could allow modular and rapid access to diversified molecules for applications such as drug and material discovery [39,40]. Based on the different reactivities of aromatic C–Br and C–Cl bonds demonstrated in homogeneous transition-metal-catalyzed couplings [41], the chemical selectivity of Cu@L6 was evaluated in tandem heterogeneous couplings

in a one-pot fashion as shown in Scheme 2. As promoted by visible-light irradiation, the Cu-catalyzed C–N coupling could be successfully conducted at 40 °C *via* the C–Br bond cleavage. After reaction, the second nucleophile was subsequently added into the reaction mixture without additional catalyst or base, which enabled the further transformation of the C–Cl bond at 80 °C exposing to the same light irradiation. The tandem reactions successfully generated unsymmetrically substituted aromatic diamines in high isolated yields (86%–95%) from conjunctive dihalides [42], which has been rarely demonstrated with heterogeneous copper catalyst.

The recycling stability of heterogeneous catalyst Cu@L6 was further examined in the reaction of 4-*n*-butyl-chlorobenzene and aqueous ammonia (Table 2). After reaction, Cu@L6 was separated from the reaction mixture simply *via* filtration, and rinsed with solvents. During 6 times of recycling experiments, the catalyst provided consistent isolated yields for 4-*n*-butylaniline. In addition, less than 1 ppm of Cu was detected in the obtained solutions, highlighting the advantages of ease-of-separation and low metal contamination of heterogeneous catalyst.

In conclusion, we have developed a novel highly porous heterogeneous polymeric catalyst, enabling visible-light promoted Cu-catalyzed C–N bond formation and tandem reaction with (hetero)aryl chlorides and various nitrogen nucleophiles under mild conditions for the first time. This method allows the synthesis of a broad scope of primary or secondary (hetero)aryl amines at good to excellent yields, and is compatible to various functional groups. Furthermore, the heterogeneous feature has facilitated the catalyst separation and recycling during multiple times of use, enabling transition-metal catalysis with low metal-contamination without extra purification. Given the importance of C–N bond formation and increasing interest in sustainable chemistry, the photo-promoted heterogeneous reaction mode



Scheme 2 Cu@L6 catalyzed tandem C-N coupling of conjunctive dihalides. Conditions: Br-R¹-Cl (0.5 mmol), R²-NH₂ and R³-NH₂ (amine=0.51 mmol; aqueous ammonia=1.0 mmol), Cu@L6 (0.05 mmol), K₃PO₄ (1.2 mmol), DMSO (0.5 mL), visible light at 405 nm. Isolated yields are based on Br-R¹-Cl (color online).

Table 2 Recycling experiments of Cu@L6 catalyzed C-N coupling^{a)}

Run	Light irradiation	Time (h)	GC yield	Isolated yield
1	405 nm	48	>99	>99
2	405 nm	48	>99	99
3	405 nm	48	99	99
4	405 nm	48	99	98
5	405 nm	48	99	97
6	405 nm	48	98	97

a) Conditions: 4-*n*Bu-Ph-Cl (0.5 mmol), aqueous ammonia (1 mmol), Cu@L6 (0.05 mmol), K₃PO₄ (0.6 mmol), DMSO (0.5 mL), 80 °C.

would provide new opportunities for catalyst design and benefit related synthesis.

Acknowledgements This work was supported by the National Natural Science Foundation of China (21704016, 21971044).

Conflict of interest The authors declare no conflict of interest.

Supporting information The supporting information is available online at <http://chem.scichina.com> and <http://link.springer.com/journal/11426>. The supporting materials are published as submitted, without typesetting or editing. The responsibility for scientific accuracy and content remains entirely with the authors.

- Horton DA, Bourne GT, Smythe ML. *Chem Rev*, 2003, 103: 893–930
- Cooper TWJ, Campbell IB, Macdonald SJF. *Angew Chem Int Ed*, 2010, 49: 8082–8091
- Devendar P, Qu RY, Kang WM, He B, Yang GF. *J Agric Food Chem*, 2018, 66: 8914–8934
- Mosrin M, Knochel P. *Chem Eur J*, 2009, 15: 1468–1477
- Evano G, Blanchard N, Toumi M. *Chem Rev*, 2008, 108: 3054–3131
- Mari M, Bartoccini F, Piersanti G. *J Org Chem*, 2013, 78: 7727–7734
- Eelkema R, Anderson HL. *Macromolecules*, 2008, 41: 9930–9933
- Ruiz-Castillo P, Buchwald SL. *Chem Rev*, 2016, 116: 12564–12649
- Surry DS, Buchwald SL. *Angew Chem Int Ed*, 2008, 47: 6338–6361
- Vo GD, Hartwig JF. *J Am Chem Soc*, 2009, 131: 11049–11061
- Ullmann F. *Ber Dtsch Chem Ges*, 1903, 36: 2382–2384
- Sambiagio C, Marsden SP, Blacker AJ, McGowan PC. *Chem Soc Rev*,

- 2014, 43: 3525–3550
- 13 Senra JD, Aguiar LCS, Simas ABC. *Curr Org Synth*, 2011, 8: 53–78
- 14 Lipshutz BH. *Chem*, 2018, 4: 2004–2007
- 15 Dery S, Kim S, Haddad D, Cossaro A, Verdini A, Floreano L, Toste FD, Gross E. *Chem Sci*, 2018, 9: 6523–6531
- 16 Ye R, Zhao J, Wickemeyer BB, Toste FD, Somorjai GA. *Nat Catal*, 2018, 1: 318–325
- 17 Li XF, Yu SB, Yang B, Tian J, Wang H, Zhang DW, Liu Y, Li ZT. *Sci China Chem*, 2018, 61: 830–835
- 18 Chen F, Li W, Sahoo B, Kreyenschulte C, Agostini G, Lund H, Junge K, Beller M. *Angew Chem Int Ed*, 2018, 57: 14488–14492
- 19 Lee JS, Kapustin EA, Pei X, Llopis S, Yaghi OM, Toste FD. *Chem*, 2020, 6: 142–152
- 20 Handa S, Wang Y, Gallou F, Lipshutz BH. *Science*, 2015, 349: 1087–1091
- 21 Hirai Y, Uozumi Y. *Chem Asian J*, 2010, 5: 1788–1795
- 22 Baig RBN, Nadagouda MN, Varma RS. *Green Chem*, 2014, 16: 4333–4338
- 23 Creutz SE, Lotito KJ, Fu GC, Peters JC. *Science*, 2012, 338: 647–651
- 24 Kainz QM, Matier CD, Bartoszewicz A, Zultanski SL, Peters JC, Fu GC. *Science*, 2016, 351: 681–684
- 25 Feng Z, Zeng T, Xuan J, Liu Y, Lu L, Xiao WJ. *Sci China Chem*, 2016, 59: 171–174
- 26 Chen Z, Lu F, Yuan F, Sun J, Du L, Li Z, Gao M, Shi R, Lei A. *Sci China Chem*, 2019, 62: 1497–1500
- 27 Miao M, Liao LL, Cao GM, Zhou WJ, Yu DG. *Sci China Chem*, 2019, 62: 1519–1524
- 28 Kibriya G, Ghosh D, Hajra A. *Sci China Chem*, 2020, 63: 42–46
- 29 Ziegler DT, Choi J, Muñoz-Molina JM, Bissember AC, Peters JC, Fu GC. *J Am Chem Soc*, 2013, 135: 13107–13112
- 30 Fan M, Zhou W, Jiang Y, Ma D. *Org Lett*, 2015, 17: 5934–5937
- 31 Zhou W, Fan M, Yin J, Jiang Y, Ma D. *J Am Chem Soc*, 2015, 137: 11942–11945
- 32 Chen Z, Ma D. *Org Lett*, 2019, 21: 6874–6878
- 33 Kupgan G, Liyana-Arachchi TP, Colina CM. *Langmuir*, 2017, 33: 11138–11145
- 34 Shen M, Liu H, Yu C, Yin Z, Muzzio M, Li J, Xi Z, Yu Y, Sun S. *J Am Chem Soc*, 2018, 140: 16460–16463
- 35 Rauws TRM, Maes BUW. *Chem Soc Rev*, 2012, 41: 2463–2497
- 36 Kolodziej K, Romanowska J, Stawinski J, Boryski J, Dabrowska A, Lipniacki A, Piasek A, Kraszewski A, Sobkowski M. *Eur J Medicinal Chem*, 2015, 100: 77–88
- 37 Hassan Z, Spuling E, Knoll DM, Lahann J, Bräse S. *Chem Soc Rev*, 2018, 47: 6947–6963
- 38 Haiduc I. *J Coord Chem*, 2019, 72: 2805–2903
- 39 Fyfe JWB, Seath CP, Watson AJB. *Angew Chem Int Ed*, 2014, 53: 12077–12080
- 40 Xu L, Zhang S, Li P. *Chem Soc Rev*, 2015, 44: 8848–8858
- 41 Wang E, Chen M. *Chem Sci*, 2019, 10: 8331–8337
- 42 Mikhailine AA, Grasa Mannino GA, Colacot TJ. *Org Lett*, 2018, 20: 2301–2305